frontiers | Frontiers in Earth Science

TYPE Original Research
PUBLISHED 13 September 2022
DOI 10.3389/feart.2022.1002745

OPEN ACCESS

EDITED BY
Shuai Yin,
Xi'an Shiyou University, China

REVIEWED BY
Zhenduo Zhao,
Jilin University, China
Zhicheng Zhou,
China University of Geosciences, China

*CORRESPONDENCE
Jishun Pan,
jspan123@126.com

SPECIALTY SECTION
This article was submitted to Structural Geology and Tectonics, a section of the journal Frontiers in Earth Science

RECEIVED 25 July 2022
ACCEPTED 15 August 2022
PUBLISHED 13 September 2022

CITATION
Pan J and Peng Y (2022), Experimental evaluation of microscopic pore structure and fluid migration characteristics of coal-measure sandstone reservoirs.
Front. Earth Sci. 10:1002745.
doi: 10.3389/feart.2022.1002745

Experimental evaluation of microscopic pore structure and fluid migration characteristics of coal-measure sandstone reservoirs

Jishun Pan* and Yicong Peng

College of Geosciences and Engineering, North China University of Water Resources and Electric Power, Zhengzhou, China

Research on the microscopic migration characteristics of fluids in coal measure sandstone has always been a hot spot in the evaluation of reservoir properties. In this study, taking the Yan'an Formation sandstone reservoirs in the Block A of the Ordos Basin as an example, the pore structures and fluid migration characteristics of coal-measure sandstones are systematically studied using a large number of thin sections, SEM (Scanning Electron Microscope), NMR (Nuclear Magnetic Resonance), relative permeability and water-flooding test results. The results show that the Jurassic sandstones in the target layer mainly develop lithic quartz sandstone, and the main pore types are intergranular and dissolution pores, followed by a small amount of intercrystalline pores. The surface porosity of the target sandstones mainly ranges from 7.90 to 10.79%, with an average value of 8.78%. The good correlation between porosity and permeability indicates that the target layer is a pore-type reservoir. The T_2 relaxation time of the target layer is mainly distributed within 100 ms. Moreover, the reservoir of the Yan'an Formation has a high saturation of movable fluids, which is mainly distributed in 43.17–71.24%, with an average value of 56.90%. Meanwhile, samples with fractures have higher movable fluid saturations. In addition, the average irreducible water saturation of the Yan'an Formation sandstone reservoir is 35.14%, and the final oil displacement efficiency is 51.14% on average. There is a good positive correlation between the oil displacement efficiency and the co-permeability zone. As the co-permeability zone range increased from 15 to 55%, the oil displacement efficiency increased from 30 to 65%. When the cores develop fractures, they have characteristics of high permeability, high oil recovery rate, high oil displacement efficiency in the anhydrous period, low irreducible water saturation and low residual oil saturation.

KEYWORDS

Yan'an formation, sandstone reservoir, relative permeability, nuclear magnetic resonance, pore structure

Introduction

The Jurassic Yan'an Formation reservoirs in the Ordos Basin have the characteristics of small oil-bearing area, therefore, the hydrocarbons are mainly distributed in small-scale traps. The physical properties of the reservoir and the development conditions of movable fluids are important parameters that determine the final cumulative production, reservoir evaluation and production cycle of oil and gas reservoirs (Ji et al., 2014; Liang et al., 2019; Lei et al., 2020; Bai et al., 2022). These properties are not only related to the pore throat diameter, but also comprehensively affected by factors such as rock porosity, pore connectivity, particle density, particle size, sorting and diagenesis (Lai et al., 2018; Guo et al., 2020; Asante-Okyere et al., 2021; Li et al., 2021). Affected by strong compaction and cementation, the matrix permeability of sandstone reservoirs is usually low. Tight sandstone reservoirs have strong heterogeneity and strong anisotropy, and the pore structures inside the rock is not only controlled by porosity but also by fluid composition. Therefore, a quantitative evaluation of the dual medium of rock and fluid components in tight reservoirs by experimental means can provide a new idea for the prediction of sweet spots in tight sandstone reservoirs (Shanley and Cluff., 2015; Liu et al., 2018; Yang et al., 2020; Mirzaei-Paiaman and Ghanbarian., 2021; Zhao et al., 2021; Li, 2022).

In the middle and late stages of waterflooding development, there is still a lot of crude oil that cannot be recovered from the formation and becomes the remaining oil. The study of the microscopic distribution of remaining oil is an important evaluation content for improving the oil recovery of tight oil reservoirs. However, in real reservoirs, the dynamic characteristics of the oil-water mutual displacement process and the distribution of remaining oil and water cannot be directly observed, so they can only be studied by experimental simulation methods (Qiao et al., 2019; Shi et al., 2019; Vafaie et al., 2021; Jiang et al., 2022). Laboratory simulation and experiments can not only provide technical support for the enhanced oil recovery, but also can provide theoretical support for the study of the reservoir development process, especially the distribution of oil and water in the pores in the high water cut stage (Wang et al., 2018; Chen et al., 2021; Katz et al., 2021; Lan et al., 2021; Wu et al., 2021). Due to the heterogeneity of the pore structures of the reservoir, the distribution of oil and water in the rock is much more complicated. The various forms of oil-water distribution require different measures to enhance the oil recovery from the reservoir.

The water flooding experiment can visually and quantitatively display the water flooding path, rate and scale, and then reveal the displacement mechanism of the microscopic remaining oil. The key to water flooding technology lies in the establishment of reservoir microscopic model and the design of technical process for experimental testing (Li et al., 2017; Li et al., 2018; He et al., 2020; Wang et al., 2022). Obviously, the rock sample model can more truly reflect the fluid migration law inside the reservoir. In this study, taking the Yan'an Formation sandstone reservoir in Block A of the Ordos Basin as an example, the pore structures and fluid migration characteristics of coal-measure sandstone are systematically studied using a large number of thin sections, SEM, NMR, relative permeability and water-flooding test results. This study can provide a reference for the formulation of efficient development plans for similar sandstone reservoirs.

Materials and methods

Geological background

The study area is located in Block A in the west of the Ordos Basin (Figure 1). From the structural background, the study area is located in the southern part of the Tianhuan Depression (Figure 1). Affected by the thrust and nappe of the western margin of the Ordos Basin, the tectonic activity in the study area was relatively strong, and a large number of small-scale faults are developed (Liang et al., 2019). The extension length of the fault is mostly distributed in 1–15 km, and the fault was mainly formed at the end of the Yanshanian Movement (Li et al., 2017). Low-amplitude uplift traps are developed in the local strata of the Yan'an Formation, and the traps are mainly distributed between 1–6 km^2.

The stratigraphic units of the Jurassic strata in this area include the Yan'an, Zhiluo and Anding Formations, among which, the Yan'an Formation has a thickness between 220–350 m. Thick river-lake delta deposits are developed in the Middle Jurassic Yan'an Formation period. In addition, coal seams are developed in the Yan'an Formation, and the Jurassic oil reservoirs in the study area are mainly distributed in the Lower system, which is also the main research target layer of this study.

The Middle Jurassic Yan'an Formation, as the main coal and oil-bearing strata in the basin, is relatively developed in the whole basin. The lithology is mainly gray and dark gray mudstone intercalated with coal seam, yellow-gray medium and fine-grained sandstone and siltstone. Because the sandstone at the bottom of the Zhiluo Formation has a strong scouring effect on the top strata of the underlying Yan'an Formation during the deposition process, the thickness of the Yan'an Formation in some areas becomes thinner. Figure 2 shows the stratigraphic unit division of the Yan'an Formation and the vertical lithologic features of the Yan'an Formation revealed by the Well Weisha 2 (Ji et al., 2014).

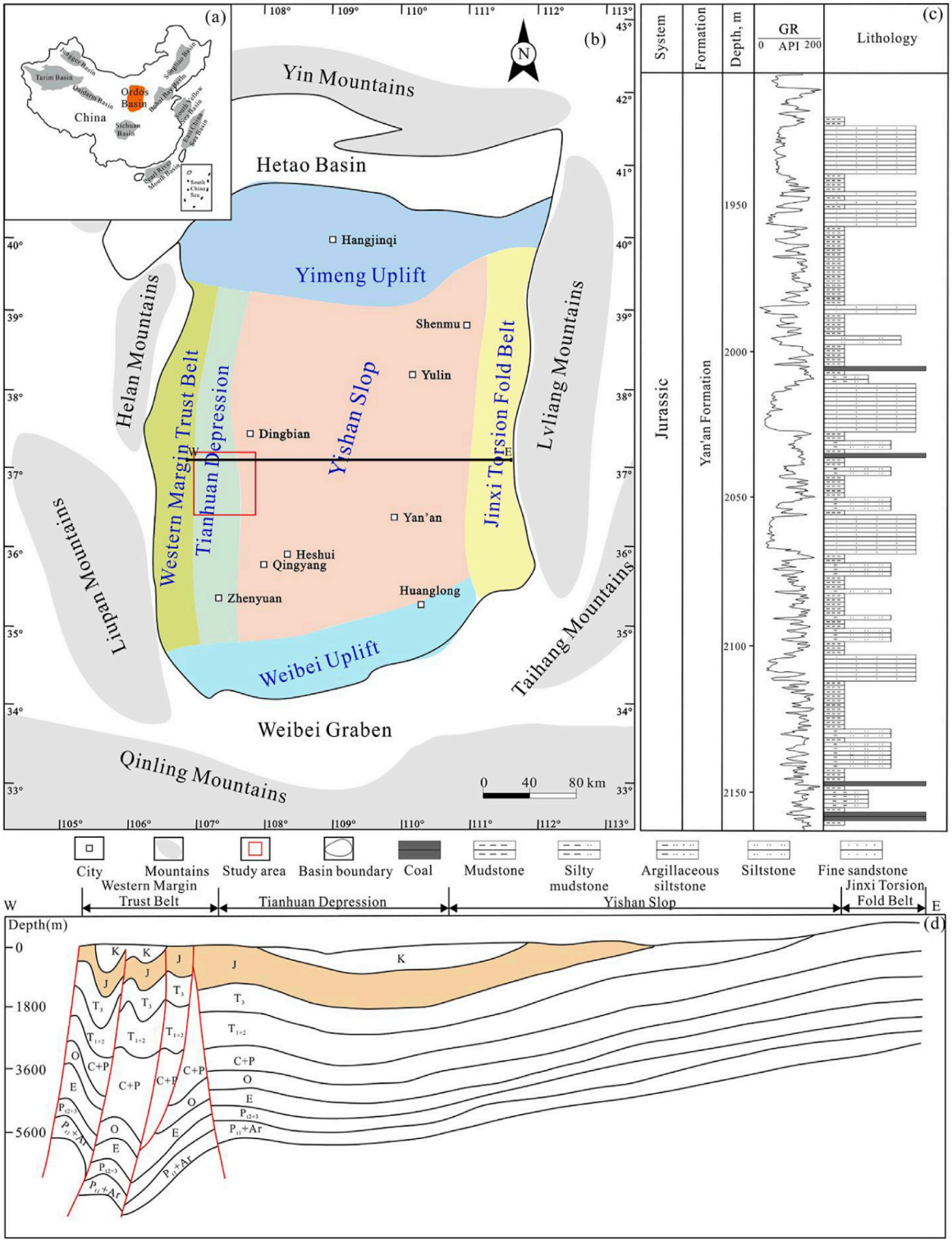

FIGURE 1
The study area is located in the western margin of the Ordos Basin in the western part of the North China Craton (NCC) (Zhong et al., 2021). Notes: **(A)** Location of the Ordos Basin; **(B)** Location of the study area; **(C)** Lithologic characteristics of the Yan'an Formation coal measures; **(D)** A stratigraphic profile in the central part of the Ordos Basin.

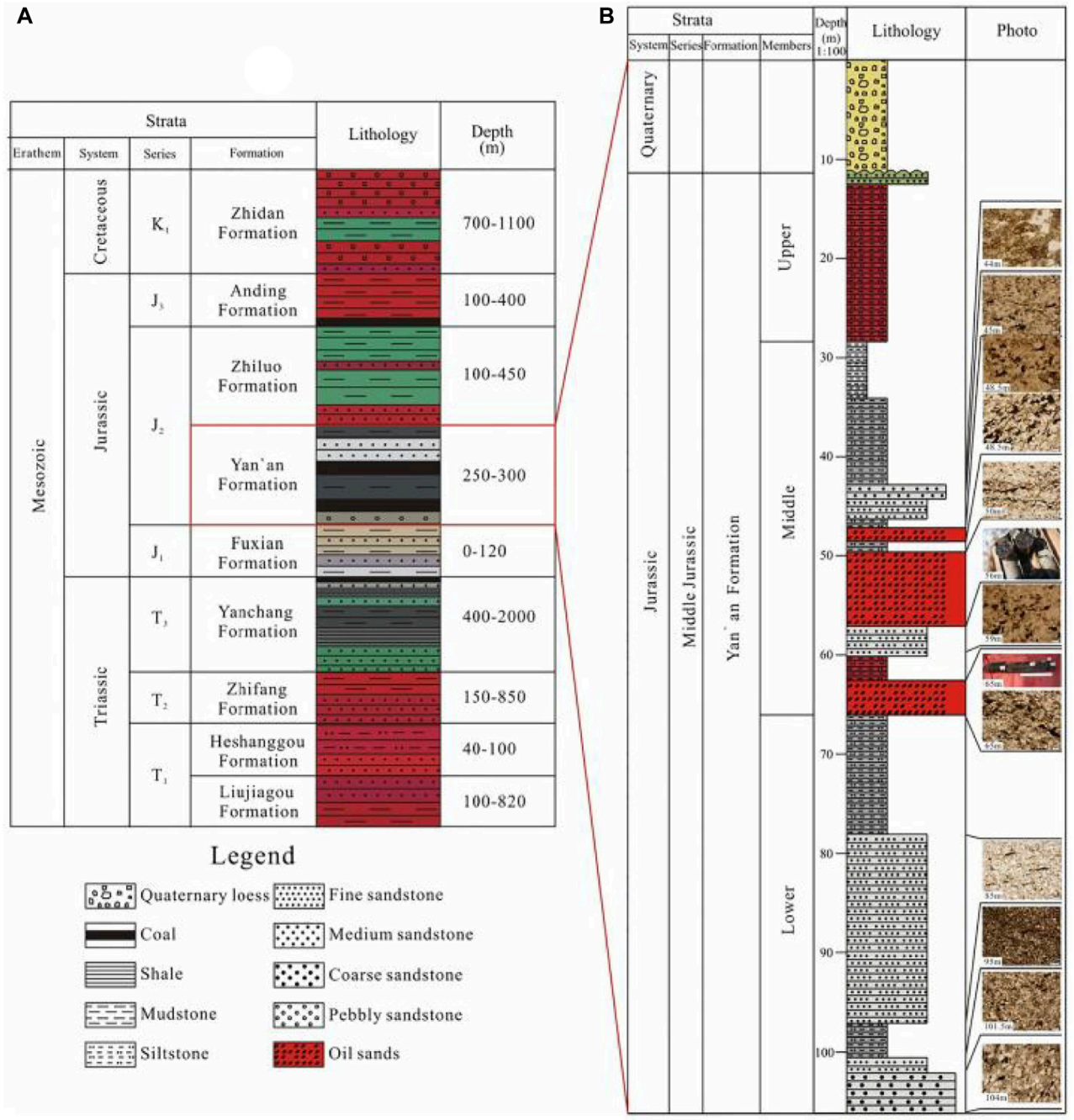

FIGURE 2
Division of stratigraphic units of the Jurassic strata in the Ordos Basin (Ji et al., 2014). Notes: **(A)** Stratigraphic units in Mesozoic strata; **(B)** Lithologic profile in Well Weisha 2.

Experiments

The experiments used in this study include thin section, scanning electron microscopy, nuclear magnetic resonance, and relative permeability tests. Thin sections and scanning electron microscopy were used to study the pore structures and the distribution of different mineral components in the sandstone. Furthermore, these experiments were used to better understand the lithology and physical properties of the Yan'an Formation sandstone.

The analysis and test of the movable fluid characteristics in this paper include nuclear magnetic resonance and relative permeability experiments. The NMR test instrument is a MagneT2000 tester. The

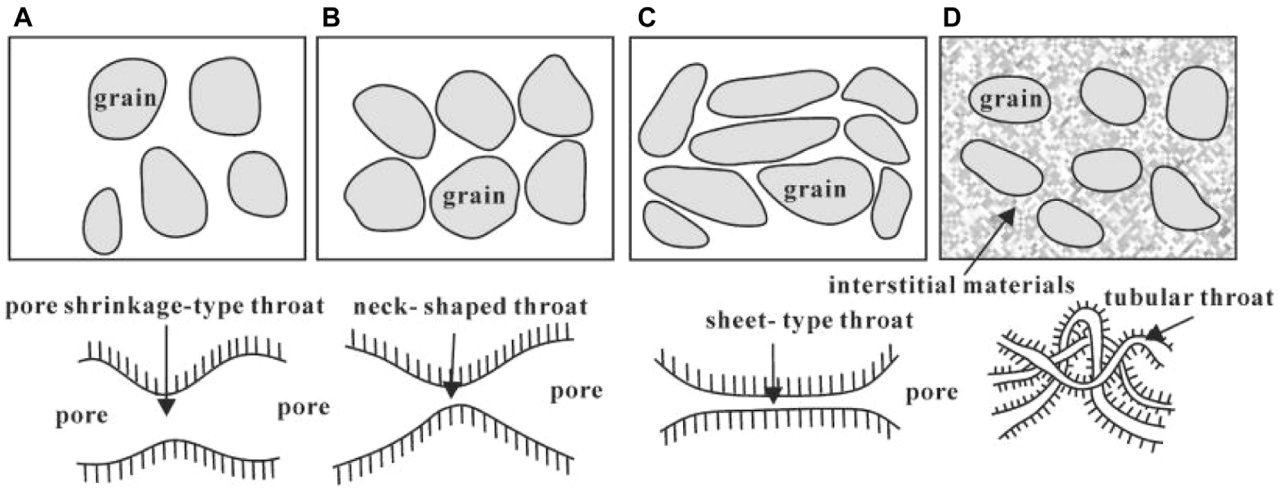

FIGURE 3
Major pore types in sandstone reservoirs (Zhong et al., 2021). **(A)** pore-shrinkage-type throat; **(B)** neck-shaped throat; **(C)** sheet-type throat; **(D)** tubular throat.

NMR test curve includes the T_2 time spectrum curve under the condition of 100% saturated formation water (before centrifugation) and the T_2 time spectrum curve after centrifugation at 450 psi. In the nuclear magnetic resonance test, the technical indicators are: the maximum working temperature is 155°C/0.5 h, the maximum working pressure is 137.9 MPa, the minimum resistivity of the drilling fluid is 0.02 Ω m, the electronic circuit AC voltage is 180 V, the frequency is 60 HZ, and the current is 250 mA. The probe DC voltage is 600 V and 800 mA/pulse. In addition, the "unsteady-state" experimental method was adopted to carry out the oil-water relative permeability test experiments on the cores. Through this test, the oil-water relative permeability curve and its characteristic parameters of the experimental samples can be obtained.

Results

Pore types

The lithologies of the Jurassic sandstones in the study area include lithic quartz sandstone, lithic feldspar sandstone and feldspar lithic sandstone. The sand bodies have poor lateral continuity, and most of the cross-sections are in the form of lenses with a flat top and a convex bottom. In addition, the sand bodies develop various types of cross-bedding, which are vertically bell-shaped and box-shaped. According to the difference of throats, the pore types of the Yan'an Formation sandstones mainly include four types (Figure 3) (Bhatti et al., 2020; Zhong et al., 2021). The first type has constricted throats with little difference in the size of pores and throats (Figure 3A); the second type has a thin-necked throat, and the size of the throats is significantly lower than the pores (Figure 3B); the third type has deformed sheet-like throats, which are associated with mineral compaction (Figure 3C); the fourth type has tubular throats, which are usually developed in the intercrystalline pores of interstitials, and the pores are mostly filled by kaolinite and illite (Figure 3D).

The observation results of casting thin section and electron microscope scanning show that there are various types of reservoir spaces in the target sandstone. The target layer mainly develops intergranular pores (Figure 4A), followed by dissolution pores and a small amount of intragranular pores. However, the dissolution pores are dominated by feldspar dissolution pores. The dissolution pores include intergranular dissolution pores, feldspar dissolution pores, detrital dissolution pores and a small amount of carbonate dissolution pores (Figure 4B).

The surface porosity of the target sandstone mainly ranges from 7.90 to 10.79%, with an average value of 8.78%. The content of residual intergranular pores in the Yan'an Formation is relatively high. Residual primary intergranular pores developed in strong hydrodynamic environments and were common in thin sections (Figure 4A). Intercrystalline pores are mainly developed in clay minerals such as kaolinite and illite. Intercrystalline pores refer to pores developed inside authigenic minerals. The larger the volume of kaolinite crystals, the better the development of intercrystalline pores (Schmitt et al., 2015; Ren et al., 2020; Zhao et al., 2020). This is due to the fact that kaolinite crystals are stacked together in a book-like form and are not sensitive to water. Therefore, a large

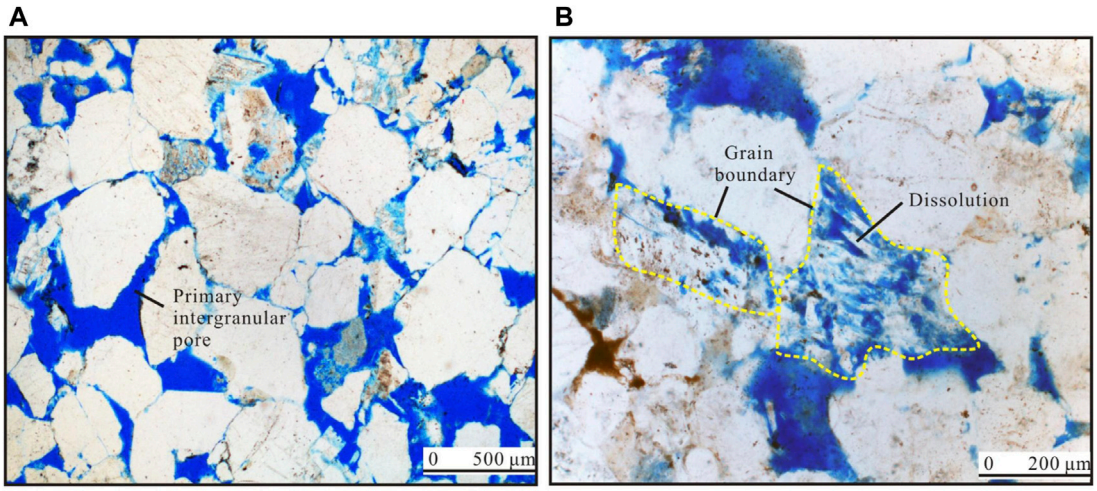

FIGURE 4
Development characteristics of pores in the target sandstone. Notes: **(A)** Well H1, 2251.4 m, detritus quartz sandstone; **(B)** Well H2, 2124.9 m, detritus quartz sandstone.

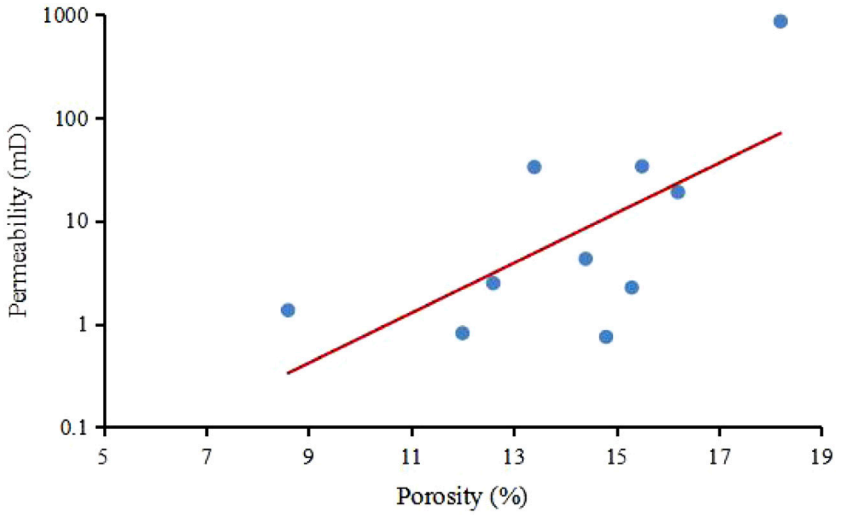

FIGURE 5
Relationship between porosity and permeability of the target layer.

number of intercrystalline pores between the crystal particles are retained.

Statistics show that feldspar has the highest degree of development of dissolved pores, and its content ranges from 0.77 to 1.55%, with an average of 1.17%. Followed by intergranular dissolved and debris dissolved pores, the content of which is distributed between 0.75 and 1.70%, with an average of 1.02%. Overall, the corrosion effect of the target layer is not strong. In addition, some micro-fractures are developed in the target layer, which can significantly improve the permeability of the reservoir.

The relationship between the porosity and gas permeability of the 10 groups of NMR samples tested is shown in Figure 5. It can be seen that there is a very good positive correlation between porosity and permeability. The porosity of the samples is mainly distributed in 9–17%, and the gas permeability is mainly

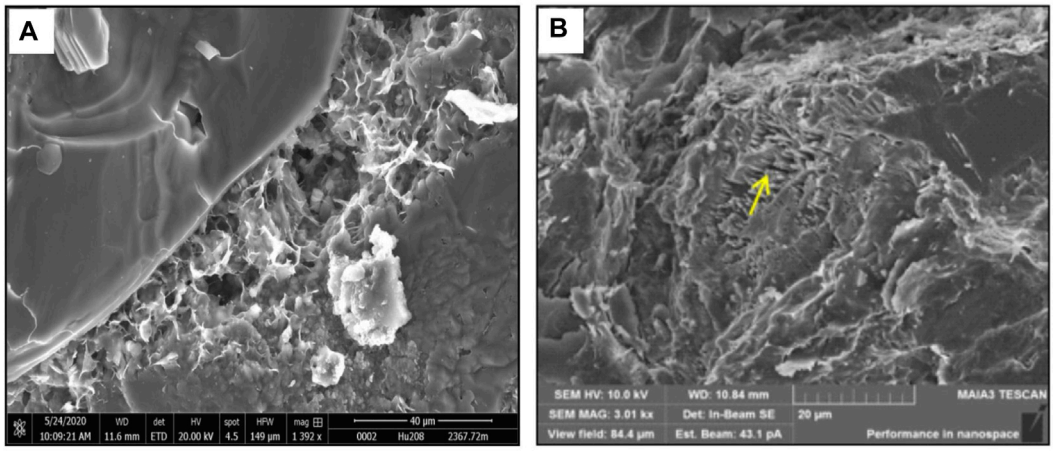

FIGURE 6
Development characteristics of clay mineral intercrystalline pores and detrital dissolution pores in the target layer. Notes: **(A)** Well X1, 2367.72 m, filamentous illite; **(B)** Well X5, 2248.13m, surface erosion of detrital particles.

distributed in 1 mD~35 mD. The target sandstone belongs to the medium-porosity and medium-permeability sandstone reservoir. The good correlation between porosity and permeability indicates that the target layer is a pore-type reservoir. Pores are mainly developed in the target layer, while fractures are less developed. The low degree of fracture development is related to the inactive tectonic activity in the Ordos Basin.

The target sandstone has experienced strong cementation. Cementation refers to the precipitation of supersaturated dissolved components in pore water under the conditions of elevated temperature and pressure, and then the clastic sediments are cemented into rocks (Wang et al., 2017; Zhong et al., 2021). The cementation experienced by the target layer mainly includes clay, siliceous, calcareous and feldspar cementations.

Statistics show that the clay cement content in the target layer ranges from 3.31 to 10.75%, with an average content of 5.65%. The authigenic clay minerals grow vertically from the pore surface to the pore center, and therefore, play a damaging role in reservoir porosity. The authigenic clay minerals in the study area are mainly kaolinite, illite, and a small amount of illite/smectite mixed layer and chlorite (Figure 6A).

Dissolution mainly occurs in the mature stage of organic diagenetic evolution, which is often consistent with the rapid transformation of smectite in the smectite/smectite clay minerals. It is also the peak period of organic acid production, so secondary pores are mostly formed in the middle diagenetic A stage. Intervals with strong dissolution are often secondary pore development segments, and are more likely to form favorable reservoirs. The dissolution of various components (clasts, matrix, cement, etc.) in the sandstone promotes the formation of a large number of secondary pores (Figure 6B). The development of dissolution pores has an extremely important influence on the physical properties of the reservoir.

T_2 spectrum classification

The movable fluid saturation of the sandstone samples of the target layer in the study area is distributed between 40 and 72%, with an average value of 54%. The different peak characteristics of the saturation component NMR curves before centrifugation can reflect the proportion of pores of different sizes in the rock. In addition, the T_2 relaxation time spectra of the NMR component curves before centrifugation can also reflect the pore size. When T_2 time is less than 1 ms, it indicates micropores (pore diameter <0.1 µm); when T_2 time is between 1 and 10 ms, it indicates small pores (pore diameter is between 0.1 and 0.5 µm); when T_2 time is between 10 and 100 ms, it indicates mesopores; when T_2 time is between 100 and 1000 ms, it indicates macropores (pore diameter is between 2.5 and 10 µm); when T_2 time is greater than 1000 ms, it indicates karst caves (pore diameter >10 µm). Generally, the types of NMR curves of sandstone reservoirs can be divided into three types: unimodal, bimodal and trimodal. Through analysis, it is considered that the NMR curve of the Yan'an Formation sandstone reservoir in the study area is relatively single in peak shape, with double peaks developed (Figure 7).

According to the different pore sizes reflected by the saturation component NMR curves before centrifugation, the pore types of the target sandstone reservoirs are divided into three categories: namely, micropore-small-pore-mesopore type (the left peak is significantly larger than the right peak), small pore-mesopore type (the left peak is significantly smaller than the

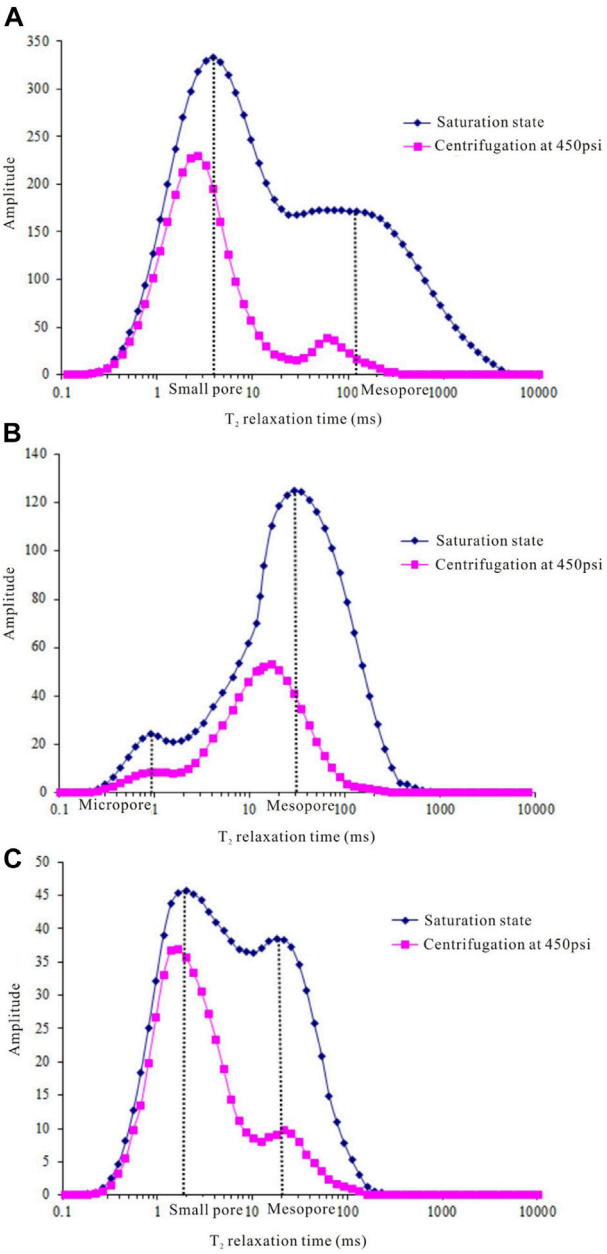

FIGURE 7
Three typical NMR curve types for Jurassic reservoirs. Notes: **(A)** Well L1, X-1 sample, 2131.7 m; **(B)** Well H4, X-2 sample, 2282.8m; **(C)** Well B8, X-3 sample, 2278.4 m.

right peak), micropore-small-pore-mesopore uniform distribution type (the left peak and the right peak have little difference).

The micropore-small-pore-mesoporous type is represented by the sample No. X-1 (Figure 7A). The saturation component curve before centrifugation shows that the T_2 relaxation time of the sample X-1 is mainly distributed in the range of 1–100 ms; the T_2 time distribution of the left peak is wider, which means that micropores and small pores dominate the rock sample. In addition, according to the coverage of the T_2 spectrum, the proportions of micropores and small pores are roughly the same. The small-mesopore type is represented by the sample No. X-2 (Figure 7B). The saturation component curve before centrifugation shows that the T_2 relaxation time of the X-2 sample is mainly distributed in the range of 10–100 ms; the T_2 time distribution of the right peak is wider, which means that the small pores and mesopores dominate the rock sample. The uniform distribution pattern of micropore-small-pore-mesopore is represented by the sample X-3 (Figure 7C). The saturation component curve before centrifugation shows that the T_2 relaxation time of the X-3 sample is mainly distributed in the range of 0.1–100 ms; and the T_2 time distribution range of the left and right peaks is wide, which means that the micropore, small pores and mesopores are well developed, and the proportion of small pores is higher on the whole.

For all samples, there is a T_2 relaxation time distribution in the interval of 100–1000 ms, but the proportion is small. It represents that a few large pores are also developed in the rock sample. In addition, there is an interval with T_2 relaxation time greater than 1000 ms in the micropore-small-pore-mesoporous samples. It shows that a few karst caves may be developed in this kind of rock samples, while no karst caves are developed in the other two types of samples.

Discussion

Analysis on the occurrence characteristics of movable fluid in coal-measure sandstone

The internal pores and throat spaces of sandstone reservoirs are narrow, and there is a certain distribution of irreducible water and movable water. Therefore, the T_2 time spectrum of NMR can be used to identify fluids with different occurrence states. The T_2 cut-off value can be determined according to the projected point value of the accumulated NMR signal intensity of the sample after centrifugation before the centrifugation (100% saturated water) on the T_2 accumulated signal intensity curve of the sample. The area covered by the post-centrifugation curve above the T_2 cut-off represents movable water, and correspondingly, the area covered by the post-centrifugation curve below the T_2 cut-off represents bound water.

The T_2 cut-off values of the sandstone samples were mainly distributed between 1 and 25 ms, with an average value of 8.24 ms. The correlation between T_2 cut-off value and porosity is not obvious. It is related to the complex pore structures of the studied sandstone and the narrow variation range of T_2 cut-off value distribution. In addition, there is a certain negative correlation between the T_2 cut-off value and the percentage of movable fluids in the rock samples. When the T_2

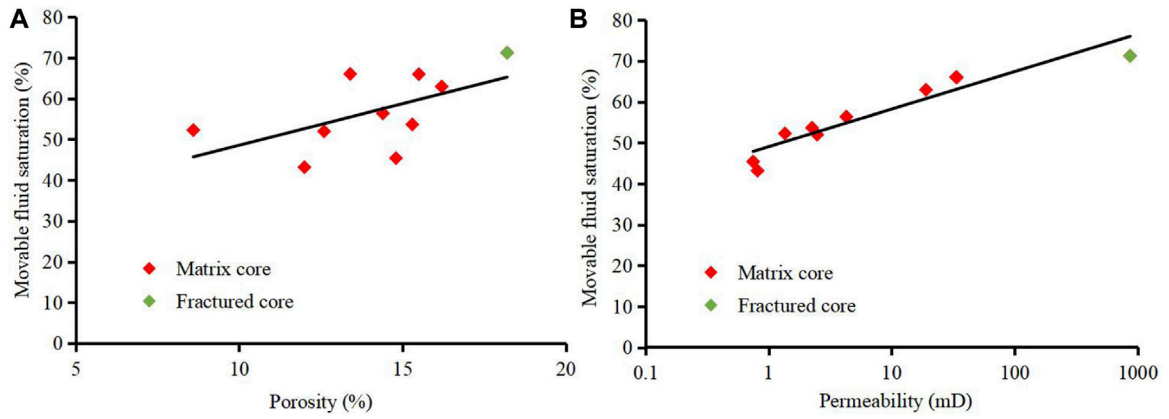

FIGURE 8
Relationship between physical parameters and movable fluid saturation of the target layer. Notes: **(A)** Relationship between porosity and movable fluid saturation; **(B)** Relationship between permeability and movable fluid saturation.

cut-off value is higher, the irreducible water saturation in the rock increases, and the corresponding percentage of movable fluid decreases. There is a very good negative correlation between mobile fluid percentage and irreducible water saturation.

Generally, the amount of movable fluid is mainly affected by the permeability of the reservoir, that is, it is mainly controlled by the throat in the reservoir space. Therefore, there is a certain positive correlation between the movable fluid content and the physical parameters. The experimental results show that the reservoir of the Yan'an Formation has high saturation of movable fluids. It was mainly distributed in 43.17–71.24%, with an average of 56.90% (Figure 8A). At the same time, the fractured samples have higher movable fluid saturations. This is because the existence of fractures greatly reduces the capillary pressure inside the tight rock, and some of the bound fluids are transformed into movable fluids. In addition, the movable fluid saturation has a significant correlation with permeability (Figure 8B). The results of well test productivity comparison show that when the movable fluid saturation is greater than 50%, the oil-producing well basically does not produce water. The tight sandstone of the Yan'an Formation has the characteristics of water wettability, and the pore surface is covered by irreducible water. The oil molecules mostly exist in a free state. Thus, high movable fluid saturation represents high oil saturation. Then, in the early stage of reservoir development, this type of reservoir only produces oil and basically does not produce water.

Analysis of relative permeability results of coal measures sandstone

For different samples, when the water saturation (S_w) changes in the same range, the oil and water relative permeability ratio K_o/K_w will change by different times, that is, the slope of the curve will be different. The smaller the slope, the smaller the change in the relative permeability ratio, and the more stable the oil and gas development effect is (Figure 9). Therefore, for the original low natural energy water-flooding reservoir, the water saturation of the tight reservoir will continue to increase with the increase of the injected water. Correspondingly, the oil-water ratio production index value will continue to decrease.

Generally, the relative permeability curve is divided into three stages: the oil phase seepage section in the state of irreducible water, the oil-water two-phase co-permeability area, and the water phase seepage in the residual oil state. Typical oil-water relative permeability curve types include Type I (concave K_w-K_o Line), Type II (descending K_o line - apex of the sloping K_w line), Type III (slowly rising K_w line - steeply falling K_o line). The target layer has the characteristics of Types I and II (Figure 10). In the oil-water two-phase seepage interval, the oil-level relative permeability of the Yan'an Formation reservoir is low. And its average residual oil saturation is 31%, and the oil-water two-phase co-seepage zone has a wide range (34% on average).

Analysis of water-flooding oil results of coal-measure sandstone

The results of water flooding experiments show that the average irreducible water saturation of the Yan'an Formation sandstone reservoir is 35.14%, and the average final oil displacement efficiency is 51.14% (Figure 11). There is a good positive correlation between the oil displacement efficiency and

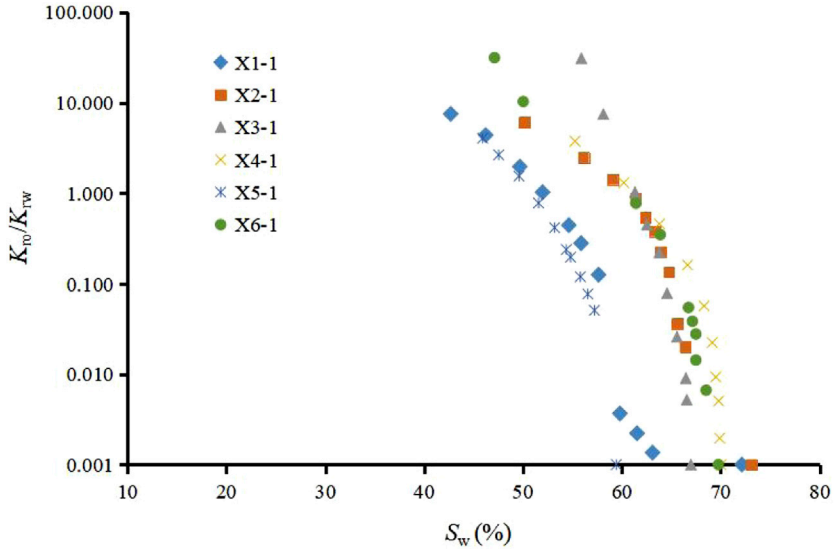

FIGURE 9
Relationship between oil-water relative permeability ratio and S_w.

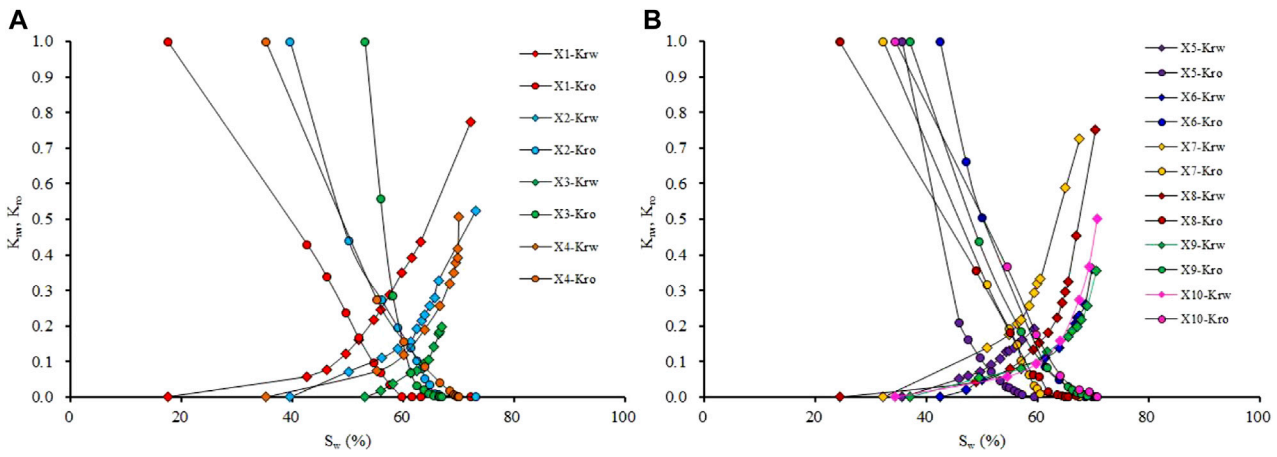

FIGURE 10
Oil-water relative permeability curves of Yan'an Formation sandstone samples. Notes: **(A)** Relative permeability curve characteristics of X1~X4 samples; **(B)** Relative permeability curve characteristics of X5~X10 samples.

the co-permeability zone (Figure 11A). As the co-permeability zone range increased from 15 to 55%, the oil displacement efficiency increased from 30 to 65%. There is a significant negative correlation between oil displacement efficiency and irreducible water saturation. That is, as the irreducible water saturation increases from 20 to 55%, the oil displacement efficiency decreases from 65 to 30%. This shows that high irreducible water content is unfavorable for oil displacement. In addition, there is a certain negative correlation between oil displacement efficiency and residual oil saturation (Figure 11C). The higher the residual oil content, the lower the oil displacement efficiency. There is a good power exponential positive correlation between oil displacement efficiency and average oil recovery rate (Figure 11D). However, if the oil production rate is too high, it will cause interlayer interference and pore pressure to drop too fast, which is not conducive to stable oil and gas production. Therefore, the oil recovery rate should be kept within a relatively reasonable range.

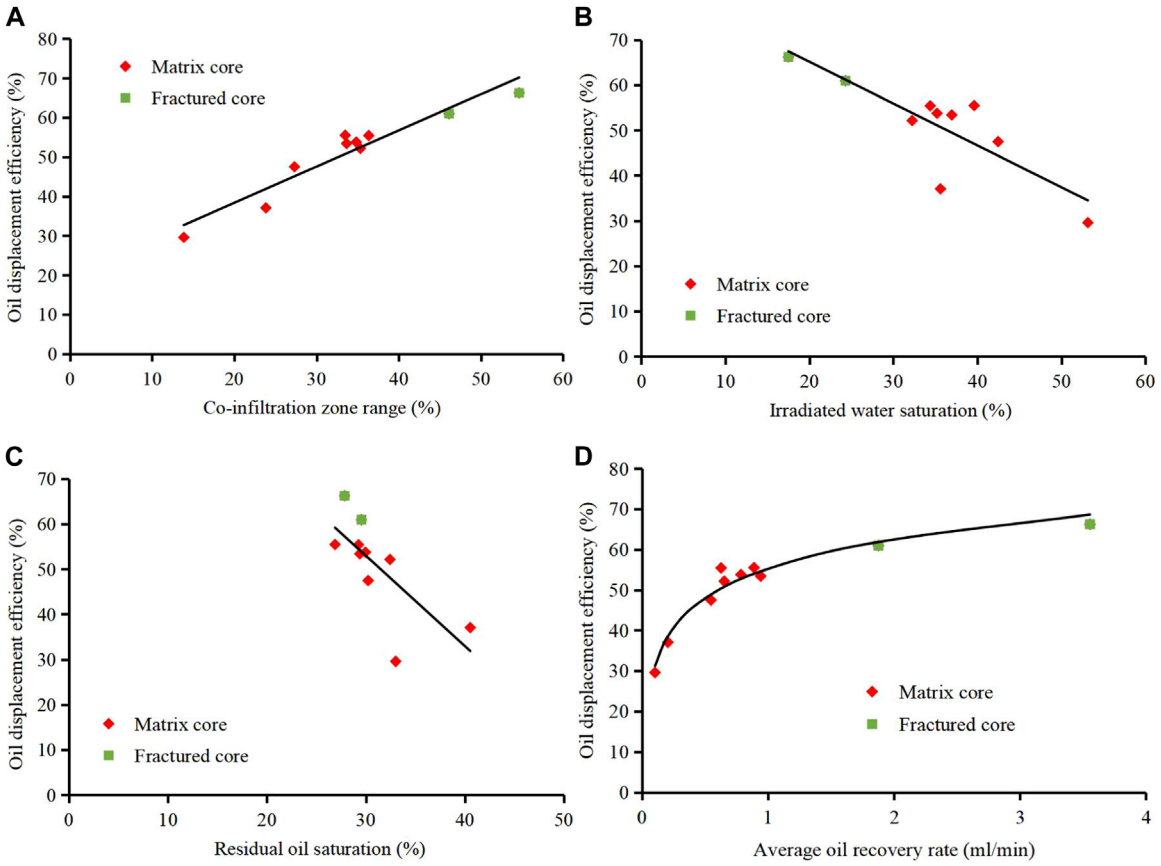

FIGURE 11
Water flooding characteristics of the target layer. Notes: **(A)** Relationship between oil displacement efficiency and co-permeability zone range; **(B)** Relationship between oil displacement efficiency and irreducible water saturation; **(C)** Relationship between oil displacement efficiency and residual oil saturation; **(D)** Relationship between oil displacement efficiency and average oil recovery rate.

This study found that when the cores have fractures, they have characteristics of high permeability, high oil recovery rate, high oil displacement efficiency in anhydrous period, low irreducible water saturation and low residual oil saturation (Figure 11). The initial productivity of the fractured samples is high, but the excessively high oil production rate can cause premature water breakthrough and reduce the productivity rapidly. At the same time, water channeling caused by fractures can form a high-speed seepage channel, which affects the displacement effect and recovery factor.

Conclusion

1) The Jurassic sandstones in the Yan'an Formation of the study area mainly develop lithic quartz sandstone, and the main pore types are intergranular and dissolution pores, followed by a small amount of intercrystalline pores. The surface porosity of the target sandstone mainly ranges from 7.90 to 10.79%, with an average value of 8.78%. The good correlation between porosity and permeability indicates that the target layer is a pore-type reservoir.
2) The T_2 relaxation time of the target layer is mainly distributed within 100 ms. The reservoir of the Yan'an Formation has high saturation of movable fluid, which is mainly distributed in 43.17–71.24%, with an average value of 56.90%. Moreover, samples with fractures have higher movable fluid saturation. In addition, the average irreducible water saturation of the Yan'an Formation sandstone reservoir is 35.14%, and the final oil displacement efficiency is 51.14% on average.
3) There is a good positive correlation between the oil displacement efficiency and the co-permeability zone. As the co-permeability zone range increased from 15 to 55%, the oil displacement efficiency increased from 30 to 65%. When the cores contain fractures, they will have characteristics of high permeability, high oil recovery rate, high oil displacement efficiency in anhydrous period, low irreducible water saturation and low residual oil saturation.

Data availability statement

The original contributions presented in the study are included in the article/Supplementary material, further inquiries can be directed to the corresponding author.

Author contributions

JP is responsible for the writing of this paper and YP is responsible for the idea of this paper.

Funding

This research was funded by the Natural Science Foundation of Xinjiang Uygur Autonomous Region—Surface Project (2019D01A34) "Accumulation Mechanism, Occurrence Characteristics and Basin Dynamics Environment of Shale (Stratification) Gas Source-Reservoir Complex".

Conflict of interest

The authors declare that the research was conducted in the absence of any commercial or financial relationships that could be construed as a potential conflict of interest.

Publisher's note

All claims expressed in this article are solely those of the authors and do not necessarily represent those of their affiliated organizations, or those of the publisher, the editors and the reviewers. Any product that may be evaluated in this article, or claim that may be made by its manufacturer, is not guaranteed or endorsed by the publisher.

References

Asante-Okyere, S., Ziggah, Y. Y., and Marfo, S. A. (2021). Improved total organic carbon convolutional neural network model based on mineralogy and geophysical well log data. *Unconv. Resour.* 1, 1–8. doi:10.1016/j.uncres.2021.04.001

Bai, J., Zhao, J., Ren, Z., Li, W., Wang, K., and Li, X. (2022). Paleogeographic and sedimentary evolution of meso–neoproterozoic strata in the Ordos Basin, Western North China Craton. *J. Petroleum Sci. Eng.* 215, 110600. doi:10.1016/j.petrol.2022.110600

Bhatti, A., Ismail, A., Raza, A., Gholami, R., Rezaee, R., Nagarajan, R., et al. (2020). Permeability prediction using hydraulic flow units and electrofacies analysis. *Energy Geosci.* 1 (1–2), 81–91. doi:10.1016/j.engeos.2020.04.003

Chen, G. B., Li, T., Yang, L., Zhang, G. H., Li, J. W., and Dong, H. J. (2021). Mechanical properties and failure mechanism of combined bodies with different coal-rock ratios and combinations. *J. Min. Strata Control Eng.* 3 (2), 023522. doi:10.13532/j.jmsce.cn10-1638/td.20210108.001

Guo, R., Xie, Q., Qu, X., Chu, M., Li, S., Ma, D., et al. (2020). Fractal characteristics of pore-throat structure and permeability estimation of tight sandstone reservoirs: A case study of chang 7 of the upper triassic yanchang Formation in longdong area, Ordos Basin, China. *J. Pet. Sci. Eng.* 184, 106555. doi:10.1016/j.petrol.2019.106555

He, X., Zhang, P., He, G., Gao, Y., Liu, M., Zhang, Y., et al. (2020). Evaluation of sweet spots and horizontal-well-design technology for shale gas in the basin-margin transition zone of southeastern Chongqing, SW China. *Energy Geosci.* 1 (3-4), 134–146. doi:10.1016/j.engeos.2020.06.004

Ji, W., Song, Y., Jiang, Z., Wang, X., Bai, Y., and Xing, J. (2014). Geological controls and estimation algorithms of lacustrine shale gas adsorption capacity: A case study of the triassic strata in the southeastern Ordos Basin, China. *Int. J. Coal Geol.* 134, 61–73. doi:10.1016/j.coal.2014.09.005

Jiang, W., Zhang, P., Li, D., Li, Z., Wang, J., Duan, Y., et al. (2022). Reservoir characteristics and gas production potential of deep coalbed methane: Insights from the no. 15 coal seam in shouyang block, Qinshui Basin, China. *Unconv. Resour.* 2, 12–20. doi:10.1016/j.uncres.2022.06.001

Katz, B., Gao, L., Little, J., and Zhao, Y. R. (2021). Geology still matters – unconventional petroleum system disappointments and failures. *Unconv. Resour.* 1, 18–38. doi:10.1016/j.uncres.2021.12.001

Lai, J., Wang, G., Wang, Z., Chen, J., Pang, X., Wang, S., et al. (2018). A review on pore structure characterization in tight sandstones. *Earth. Sci. Rev.* 177, 436–457. doi:10.1016/j.earscirev.2017.12.003

Lan, S. R., Song, D. Z., Li, Z. L., and Liu, Y. (2021). Experimental study on acoustic emission characteristics of fault slip process based on damage factor. *J. Min. Strata Control Eng.* 3 (3), 033024. doi:10.13532/j.jmsce.cn10-1638/td.20210510.002

Lei, Q., Zhang, L., Tang, H., Zhao, Y., Chen, M., and Xie, C. (2020). Describing the full pore size distribution of tight sandstone and analyzing the impact of clay type on pore size distribution. *Geofluids* 2020, 1–20. doi:10.1155/2020/5208129

Li, H. (2022). Research progress on evaluation methods and factors influencing shale brittleness: A review. *Energy Rep.* 8, 4344–4358. doi:10.1016/j.egyr.2022.03.120

Li, J., Zhang, X., Tian, J., Liang, Q., and Cao, T. (2021). Effects of deposition and diagenesis on sandstone reservoir quality: A case study of permian sandstones formed in a braided river sedimentary system, northern Ordos Basin, northern China. *J. Asian Earth Sci.* 213, 104745. doi:10.1016/j.jseaes.2021.104745

Li, P., Sun, W., Wang, Z., Huang, H., and Zhe, W. (2018). Features of microscopic pore structure and their influence on oil displacement efficiency in Chang 8^1 reservoir of Xifeng Oilfield, Ordos Basin. *Geoscience* 32 (6), 1194–1202.

Li, Z., Wu, S., Xia, D., Zhang, X., and Huang, M. (2017). Diagenetic alterations and reservoir heterogeneity within the depositional facies: A case study from distributary-channel belt sandstone of upper triassic yanchang Formation reservoirs (Ordos Basin, China). *Mar. Pet. Geol.* 86, 950–971. doi:10.1016/j.marpetgeo.2017.07.002

Liang, Y., Shan, X., Hao, G., Yousif, M., Wan, H., Habeeb, A., et al. (2019). Petrological and organic geochemical characteristics of oil sands from the middle jurassic yan'an Formation in the southern Ordos Basin, China. *Acta Geol. sinica-. Engl. Ed.* 12, 79–626. doi:10.1111/1755-6724.14203

Liu, Y., Hu, W., Cao, J., Wang, X., Tang, Q., Wu, H., et al. (2018). Diagenetic constraints on the heterogeneity of tight sandstone reservoirs: A case study on the upper triassic xujiahe Formation in the sichuan basin, southwest China. *Mar. Pet. Geol.* 92, 650–669. doi:10.1016/j.marpetgeo.2017.11.027

Mirzaei-Paiaman, A., and Ghanbarian, B. (2021). A new methodology for grouping and averaging capillary pressure curves for reservoir models. *Energy Geosci.* 2, 52–62. doi:10.1016/j.engeos.2020.09.001

Qiao, J., Zeng, J., Jiang, S., Feng, S., Feng, X., Guo, Z., et al. (2019). Heterogeneity of reservoir quality and gas accumulation in tight sandstone reservoirs revealed by pore structure characterization and physical simulation. *Fuel* 253, 1300–1316. doi:10.1016/j.fuel.2019.05.112

Ren, D., Yang, F., Li, R., Zhou, D., Liu, D., and Li, Y. (2020). Insight into the pore structures and its impacts on movable fluid in tight sandstones. *Geofluids* 2, 1–11. doi:10.1155/2020/8820023

Schmitt, M., Fernandes, C. P., Wolf, F. G., da Cunha, B., Neto, J. A., Rahner, C. P., et al. (2015). Characterization of Brazilian tight gas sandstones relating permeability and Angstrom-to micron-scale pore structures. *J. Nat. Gas. Sci. Eng.* 27, 785–807. doi:10.1016/j.jngse.2015.09.027

Shanley, K. W., and Cluff, R. M. (2015). The evolution of pore-scale fluid-saturation in low permeability sandstone reservoirs. *Am. Assoc. Pet. Geol. Bull.* 99, 1957–1990. doi:10.1306/03041411168

Shi, G., Shen, C., Zattin, M., Wang, H., Yang, C., and Liang, C. (2019). Late CretaceousCenozoic exhumation of the Helanshan Mt Range, Western Ordos fold-

thrust belt, China: Insights from structural and apatite fission track analyses. *J. Asian Earth Sci.* 176, 196–208. doi:10.1016/j.jseaes.2019.02.016

Vafaie, A., Kivi, I. R., Moallemi, S. A., and Habibnia, B. (2021). Permeability prediction in tight gas reservoirs based on pore structure characteristics: A case study from south western Iran. *Unconv. Resour.* 1, 9–17. doi:10.1016/j.uncres.2021.08.001

Wang, G., Chang, X., Yin, W., Li, Y., and Song, T. (2017). Impact of diagenesis on reservoir quality and heterogeneity of the Upper Triassic Chang 8 tight oil sandstones in the Zhenjing area, Ordos Basin, China. *Mar. Pet. Geol.* 83, 84–96. doi:10.1016/j.marpetgeo.2017.03.008

Wang, H., Alvarado, V., Mclaughlin, J. F., Bagdonas, D. A., Kaszuba, J. P., Campbell, E., et al. (2018). Low-field nuclear magnetic resonance characterization of carbonate and sandstone reservoirs from rock spring uplift of Wyoming. *J. Geophys. Res. Solid Earth* 123 (9), 7444–7460. doi:10.1029/2018JB015779

Wang, H., Zhou, S., Li, S., Zhao, M., and Zhu, T. (2022). Comprehensive characterization and evaluation of deep shales from Wufeng-Longmaxi Formation by LF-NMR technology. *Unconv. Resour.* 2, 1–11. doi:10.1016/j.uncres.2022.05.001

Wu, T., Li, L., Li, W., Gai, Y., Qiu, Y., Pan, G., et al. (2021). A quantitative study on source rocks in the Western Leidong depression, northern South China Sea. *Energy Geosci.* 2 (1), 73–82. doi:10.1016/j.engeos.2020.10.002

Yang, Y., Li, X., Zhang, Y., Mei, Y., and Ding, R. (2020). Insights into moisture content in coals of different ranks by low field nuclear resonance. *Energy Geosci.* 1 (3–4), 93–99. doi:10.1016/j.engeos.2020.05.004

Zhao, K. K., Jiang, P. F., Feng, Y. J., Sun, X. D., Cheng, L. X., and Zheng, J. W. (2021). Investigation of the characteristics of hydraulic fracture initiation by using maximum tangential stress criterion. *J. Min. Strata Control Eng.* 3 (2), 023520. doi:10.13532/j.jmsce.cn10-1638/td.20201217.001

Zhao, Z., Wu, K., Fan, Y., Guo, J., Zeng, B., and Yue, W. (2020). An optimization model for conductivity of hydraulic fracture networks in the Longmaxi shale, Sichuan basin, Southwest China. *Energy Geosci.* 1 (1–2), 47–54. doi:10.1016/j.engeos.2020.05.001

Zhong, X., Zhu, Y., Jiao, T., Qi, Z., Luo, J., Xie, Y., et al. (2021). Microscopic pore throat structures and water flooding in heterogeneous low-permeability sandstone reservoirs: A case study of the jurassic yan'an Formation in the huanjiang area, Ordos Basin, northern China. *J. Asian Earth Sci.* 219, 104903. doi:10.1016/j.jseaes.2021.104903